Control of the growth of electrodeposited zinc oxide on FTO glass

Hajar Ghannam, Cyrille Bazin, Adil Chahboun, Mireille Turmine

ARTICLE

Control of the growth electrodeposited Zinc oxide onto FTO glass

Hajar Ghannam[a,b], Cyrille Bazin[a], Adil Chahboun[b], Mireille Turmine*[a]

In this work, zinc oxide (ZnO) was directly electrodeposited onto Fluorine-doped tin oxide (FTO). The physical and chemical heterogeneity of FTO have contributed to important and exploitable results. In fact, the doping of tin dioxide (SnO_2) with fluorine distorts its rutile crystal lattice. This distortion leads to contraction mechanical constraints on the network contributing to a rough surface morphology. Moreover, the nano-roughness of FTO surface impedes the epitaxial growth of ZnO nanorods. However, this roughness combined with the chemical heterogeneity of the FTO surface leads to favored growth sites. This can be explained by the presence of fluorine atoms, into the SnO_2 network, with a stronger electronegativity which attracts the ZnO nuclei. The accumulation of many nuclei around the same electronegative spot contributes to the development of nanoflower-like structures or tilted nanorods. In such case, the non-polar facets of ZnO are exposed and the electrodeposited film is highly hydrophobic. The growth of ZnO onto FTO was studied by varying four main parameters of the synthesis: time of electrodeposition, temperature, concentration of Zn^{2+} precursor and concentration of KCl. The influence of those parameters on the shape, size, growth mechanism, and density of the ZnO electrodeposit was discussed. Thus, when the concentration of Zn^{2+} precursor increases from 0.1 to 5 mM, the nanorods' size decreases but the density of these nanostructure increases leading to their organization in nanoflowers. However, the increase of KCl concentration from 0.5 to 4 M causes a change of the ZnO nanostructures shape from hexagonal nanorod arrays to nanopencil arrays and also a significant decrease of density accompanied with a significant increase of ZnO nanostructures size whose diameter varies from 90 to 200 nm. Furthermore, the time of electrodeposition is a key parameter influencing the height of ZnO nanorods. Finally, a good crystallization of ZnO is observed at high temperature (about 80°C).

1. Introduction

Zinc oxide (ZnO) is a low cost and non-toxic material. It has a large band gap (3.3 eV) absorbing UV rays hence its application as an anti-UV coating[1]. It is used, also, in the absorber layer for photovoltaic applications[2]. The structural property of ZnO thin films has a major influence on the observed change of its electrical, optical, photocatalytic and wettability properties.[3-12] These properties can be improved or weakened according to the nanostructures size. In fact, when the nano-roughness of ZnO film decreases, conductivity and photocatalytic activity decrease, on the other hand the transmittance increases.[13, 14] Moreover, the nanostructures influence the wettability behavior of a surface, playing an amplifier role. A hydrophobic surface becomes super-hydrophobic when nano-roughness increases and vice versa.[15] Therefore, the study of ZnO nanostructures is very important, since many properties depend on their shape and/or size. ZnO nanostructures can be grown in forms of nanoplates, nanoflowers, nanorods, nanotubes[16], etc. ZnO nanorod is one of the more interesting form for photovoltaic application thanks to the large surface area.[17] The geometric features of ZnO nanorods depend on synthesis technique and deposition condition. Electrochemical technique is the most efficient method for tuning structural properties.[18] Several studies were carried out in aim to control the growth

of ZnO using electrochemical method by varying the concentration and nature of supporting electrolyte, or the concentration of the precursors (Zn^{2+} and OH^-). Skompska et al.[19] have presented an extensive review about electrodeposition of ZnO nanorod arrays on transparent conducting substrates. Tena-Zaera et al.[20] have studied the effect of supporting electrolyte concentration (potassium chloride) on the ZnO nanostructure electrodeposited onto Fluorine-doped Tin Oxide (FTO) first covered by a seed layer of ZnO nanocrystallite. They showed that the increase of KCl concentration causes a rise of ZnO deposition efficiency. Furthermore, for a high concentration of KCl (>1M) a lateral growth of ZnO is favored. Elias et al.[21] have investigated the effect of the anion nature of the supporting electrolyte on the features of the ZnO nanostructures, showing that the change of anion nature leads to a difference in adsorption behavior onto ZnO nanostructures, causing a variation on OH-production rate and therefore a modification of ZnO nanostructure sizes. In fact, several studies have been focused on the effect of the concentration of Zn^{2+} precursor on ZnO nanostructure growth, finding that the concentration of Zn^{2+} precursor is the major parameter influencing the ZnO geometric dimensions; the size of ZnO nanostructures increases when concentration of Zn^{2+} precursor rises.[22] Other parameters, as time and temperature of the electrodeposition, were studied.[23, 24]

In this work, we have explored the effect of electrosynthesis parameters on the ZnO growth on FTO. Contrarily to the majority of the published studies, we made the choice to electrodeposit the ZnO thin layer directly on FTO surface in order to simplify the operating mode and to benefit from the surface nature of the FTO. Most often, only one characteristic

[a] Sorbonne Université, CNRS, Laboratoire Interfaces et Systèmes Electrochimiques (LISE), 75005 Paris, France
[b] Abdelmalek Essaadi University, FST Tanger, laboratoire des Nanomatériaux et Couches Minces (NCM), 90000 Tangier, Morocco
*corresponding author: mireille.turmine@upmc.fr

ARTICLE   **Journal Name**

is sought such as maximum of hydrophobicity[25] and few studies have considered the variations of the experimental conditions on the morphology of ZnO nanostructures directly deposited on the FTO. Xu et al.[26] have examined the effect of some additives in order to control the ZnO nanostructures growth and especially they sought the better conditions to obtain compact epitaxial growth of ZnO nanostructures. In our case, we provided four main parameters: the concentration of Zn^{2+} precursor, concentration of supporting electrolyte KCl, time and temperature of electrodeposition. The variations of these key parameters modified the morphology of ZnO nanostructures and the growth mechanism.

2. Experimental

ZnO was successfully electrochemically deposited by using three-electrode classical cell. FTO glass (from Solems, 80 nm thickness), a saturated calomel electrode (SCE) and a Zinc rod was used as working electrode (WE), reference electrode (RE) and counter electrode (CE), respectively. FTO was cleaned prior any use with acetone and ethanol, for 10 min each, in an ultrasonic bath, afterwards it was rinsed with distilled water.

To deposit ZnO, the three electrodes (CE, WE and RE) were vertically immersed in an aqueous electrolyte containing $ZnCl_2$ (MERCK, purity>95%) as a source of Zn^{2+}, gaseous dioxygen (O_2) as OH^- precursor and KCl (VWR International, purity 99.0-100.5%) was used as supporting electrolyte to increase the electrical conductivity of the solution. The temperature of the solution was kept constant using a cryostat bath.
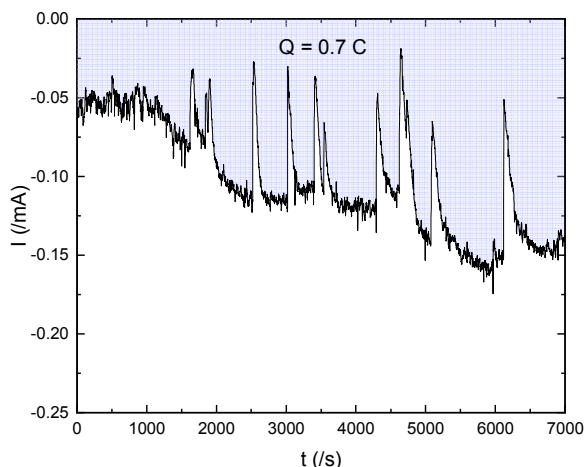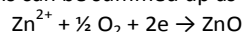

Fig. 1 The chronoamperograms for the preparation of ZnO nanostructure on FTO at −1.0 V/SCE during 7000s in a O_2 saturated aqueous medium of 2.5 mM $ZnCl_2$ and 0.1 M KCl.

The electrodeposition of ZnO is generally realized by an elevation of the local pH, due to the reduction of the oxygen in

order to provide hydroxides around the surface. Then, the formation of metal oxide is made by chemical reaction between the native hydroxides (OH^-) and the metal cations present in the solution, according to the following reactions under static-potential (E = -1V/SCE):

$O_2 + 4e + 2\ H_2O \rightarrow 4\ OH^-$

$Zn^{2+} + 2\ OH^- \rightarrow ZnO + H_2O$
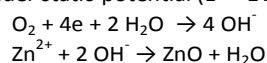
This can be summed up as

$Zn^{2+} + \frac{1}{2}\ O_2 + 2e \rightarrow ZnO$

The quantity of ZnO deposited on the cathode was estimated from the total electric charge, Q (in Coulombs). The latter was calculated from the integration of the chronoamperometric curve (Fig. 1). From the Faraday's law, one can write

$$m = \frac{Q \times M}{z \times F} \qquad (eq.1)$$

In which, m is the mass of ZnO electrodeposited on the WE (FTO), F (= 96500 C mol^{-1}) is the Faraday constant, z is the number of transferred electrons per ion which is equal to 2, and M is the molar mass of ZnO (81.38 g mol^{-1}).

The morphology of the electrosynthesized ZnO thin films was analyzed by field emission scanning electron microscope (SEM-FEG) ULTRA 55 ZEISS. The crystal structure of ZnO thin films was investigated by *Empyrean Panalytical* X-ray diffraction (XRD).

3. Results and discussion

To study the ZnO growth on FTO substrate, four main parameters (concentration of Zinc precursor, of the supporting electrolyte KCl, time and temperature of electrodeposition) were changed during the ZnO electrosynthesis.

3.1 Effect of $ZnCl_2$ concentration on ZnO nanorods growth onto FTO

Several aqueous solutions containing the same KCl concentration (0.1 M) but different concentrations of $ZnCl_2$ (between 0.1 to 5 mM) were prepared. All these solutions were saturated with oxygen by bubbling. The electrodeposition of ZnO on FTO was performed at 80°C during 1000s at -1 V/SCE. The SEM pictures (Fig. 2) show that at low $ZnCl_2$ concentration (< 0.5 mM), the nanorods of ZnO are gathered in 2-3 nanorods. For high concentrations of $ZnCl_2$ (> 0.5 mM), the number of amassed nanorods increases leading to a nanoflower shape. Therefore, the density of nano-columns increases when the concentration of $ZnCl_2$ increases. For a concentration of 0.1mM the density is about 21 nanorods/μm^2 and for a concentration of 5mM the density is about 73 nanorods/μm^2.
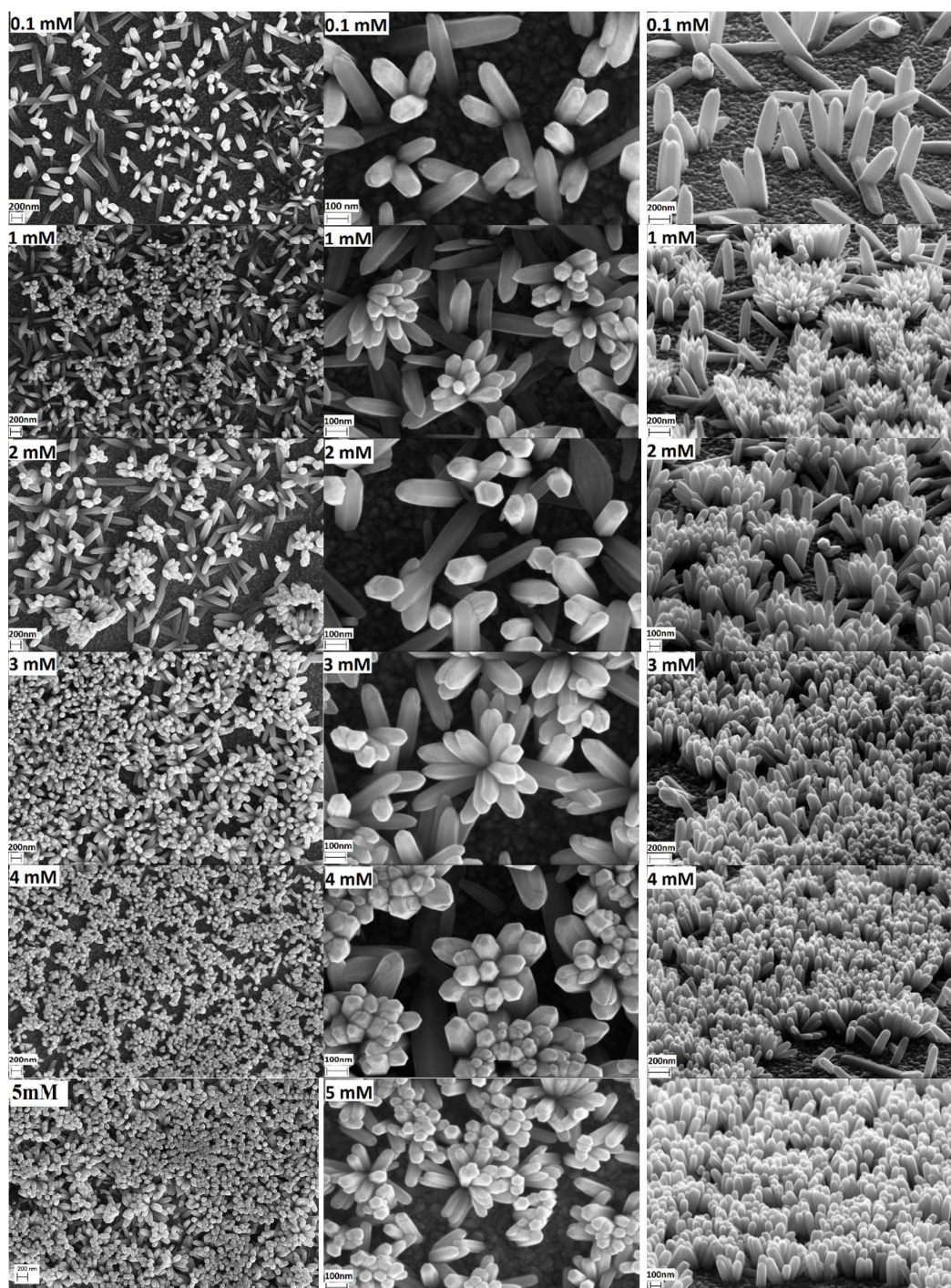
Journal Name

ARTICLE

Fig. 2 SEM images of ZnO nanorods (plan and cross-sectional views) obtained in different ZnCl$_2$ concentrations, at 80°C, during 1000 s, at E=-1V/SCE, in 0.1M KCl.

The polarity of underlying surface plays a main role on the apparition regions of ZnO nanostructures, as illustrated by Lee *et al*.[27] and Perillat-Merceroz *et al*.[28] who generated a selective growth of ZnO by controlling the surface polarity. In our case, this underlying surface polarity can explain the observed ZnO growth. The difference in electronegativity between FTO atoms generates some more welcoming regions for ZnO deposition.

Hence, due to its polarity, the first nucleus of ZnO choose fluorine atom to be linked to the surface through its Zn-polar facet. The number of nuclei linked to the surface depends on the zinc precursor concentration; a high concentration of Zn^{2+} precursor gives rise to a high density of ZnO nuclei around the same region contributing after growth process to nanoflower form (Fig. 3).

ARTICLE

Journal Name

Contrariwise the density, the height and width of ZnO nanorods decrease when the concentration of $ZnCl_2$ increases. Thus, when the $ZnCl_2$ concentration increases from 0.1 to 5mM, we found a
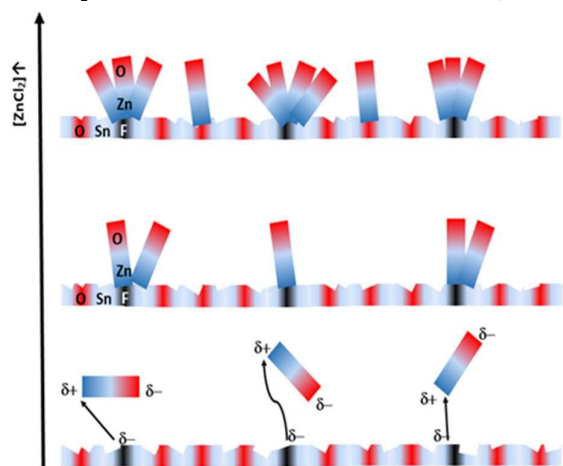

Fig. 3 Schematic illustration of ZnO growth mechanism for different concentrations of $ZnCl_2$.

diminution in height and width (Fig. 4). This reduction in size of ZnO nanorods is accompanied by mass loss (Table 1). The mass of ZnO deposited on FTO increases when concentration of $ZnCl_2$ varies from 0.1 to 1 mM and decreases for concentration of $ZnCl_2$ higher
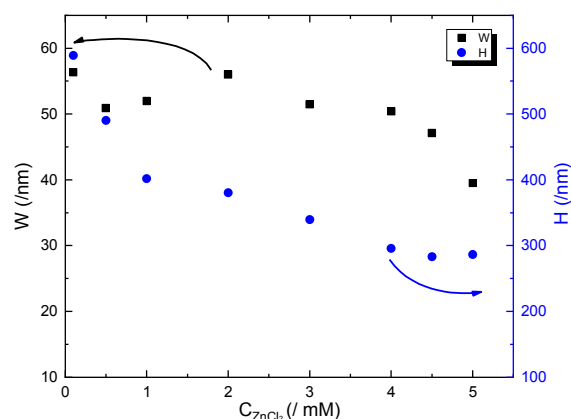

Fig. 4 Mean values of nanorod dimensions as a function of $ZnCl_2$ concentration, black squares for the width (W) and blue circles for the height (H).

than 1mM (Table 1). This reduction of mass and size can be justified by the inequality between diffusion coefficient of molecular oxygen and Zn^{2+}.[29, 30] The diffusion coefficient of molecular oxygen is more important than Zn^{2+} what makes the production of OH^- ions faster than the transport of Zn^{2+}. The OH^- ions produced at the electrode diffuse towards the bulk solution through the ZnO nanostructures and adsorb on nanorod tips. The adsorption phenomenon of OH^- ions weakens the polarity of ZnO and therefore its growth. Moreover, we have to notice that our results are different from those presented by Elias *et al.*[22] This is mainly related to the surface polarity. Elias *et al.* have studied the effect of concentration of Zn^{2+} precursor on ZnO growth on FTO first covered by a buffer layer of ZnO finding that the size of ZnO nanorods increases with the concentration of Zn^{2+} precursor in the solution. The coating of FTO surface by smooth ZnO layer before depositing the ZnO nanorods

leads to a surface polarity equilibrium forming a homogeneous and well-dispersed deposit of ZnO nanorods.

[$ZnCl_2$] /(mM)	Charge density (/C cm^{-2})	m(ZnO) (/µg)
0.1	0.136	57
0.5	0.197	83
1	0.199	84
2	0.165	70
3	0.160	67
4	0.150	63
5	0.145	61

Table 1 Estimated values of mass for electrodeposited ZnO nanorods according to the concentration of zinc precursor.

3.2 Time effect on ZnO nanorods growth on FTO

Several ZnO samples were prepared from solution of 0.1M KCl and 2.5mM $ZnCl_2$ saturated with oxygen by bubbling. The electrodeposition of ZnO is realized at 80°C, constant potential (-1V/ SCE) and for an electrodeposition time varying between 0 and 10000s.

Fig. 5 depicts some SEM images of different ZnO growths on FTO surface as a function of the electrodeposition time. The dimension values of ZnO nanorods estimated from SEM images are gathered in Fig. 6. As shown on Fig. 5, the density of ZnO nanorods increases until time of 2000s. While, the density remains almost constant ($\approx$ 20 nanorods/μm^2) for a deposition time higher than 2000s. If we focused on the nanostructures size, we can notice that the width increases in the first moment and then remains constant (around of 78nm) from an electrodeposition time of 3000s. Regarding the height variation of ZnO nanorods, a monotonous increase over the time was observed, it goes from 300nm for 500s to 1100nm for 10000s. Moreover, as seen on Table 2, the mass of electrodeposited ZnO on FTO increases as a function of time.

Time (/s)	Charge density (/C cm^{-2})	m (ZnO) (/µg)
500	0.048	20
1000	0.1447	61
2000	0.181	76
3000	0.273	115
4000	0.379	160
5000	0.479	202
6000	0.600	253
7000	0.700	295
8000	0.825	348
9000	0.943	398
10000	1.070	451

Table 2 Estimated values of mass of electrodeposited ZnO nanorods as a function of time

The growth of ZnO on the rough FTO surface probably begins by the appearance of nuclei of ZnO on the anfractuosities due to the surface roughness. Those first nuclei adopt the same inclination angle than FTO nano-roughness hence the appearance of inclined nanorods of ZnO. Ichinose *et al.*[31] had discussed the influence of surface roughness on the ZnO orientation. Moreover, ZnO growth along *c* axis is mainly related to its crystal structure. The Wurtzite crystal structure

Journal Name

ARTICLE

of ZnO is non-centrosymmetric. The absence of symmetry center leads creating a dipole moment in the ZnO crystal lattice along the c axis which causes an instability of ZnO O-polar facet (0001).
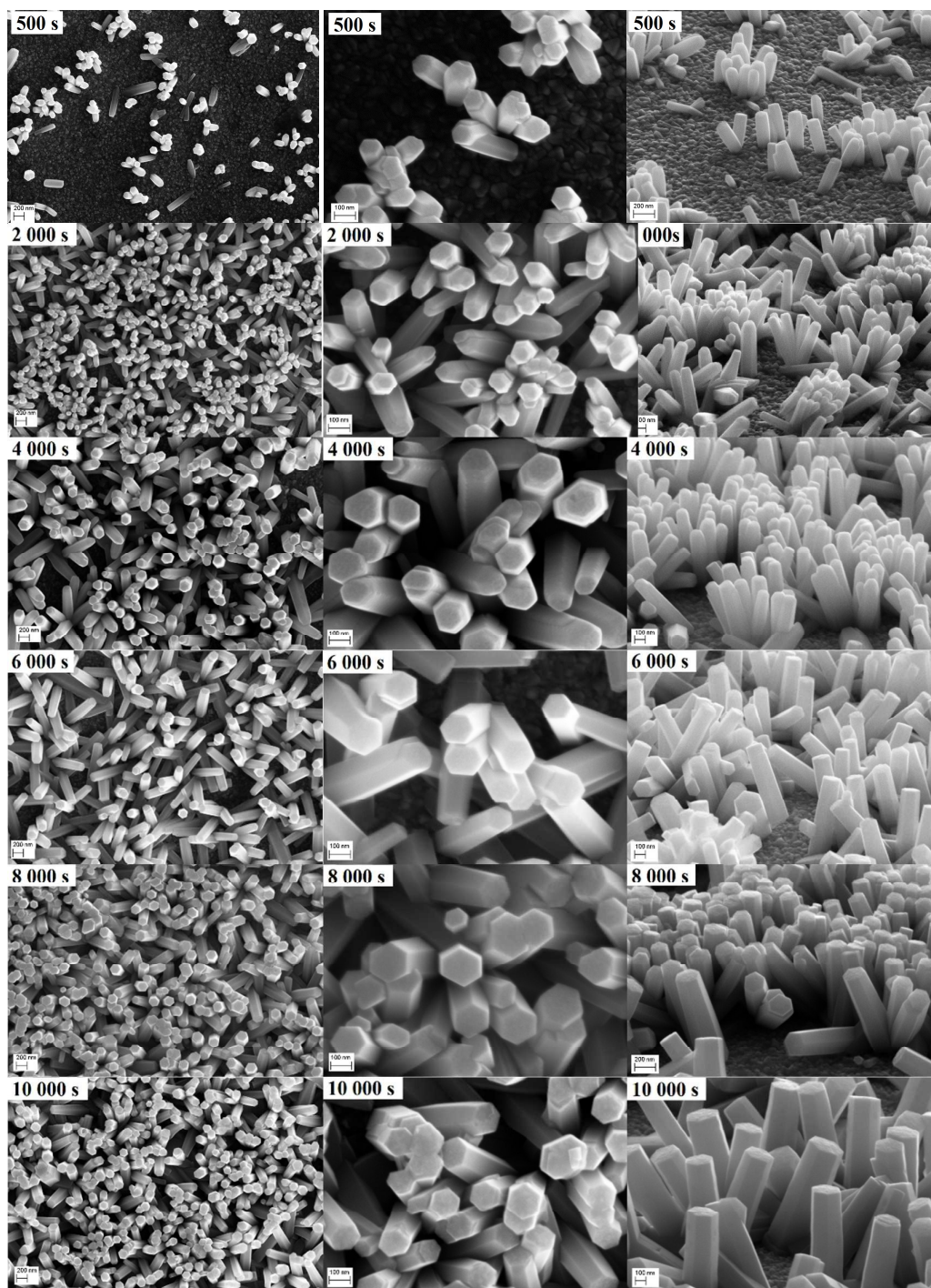

Fig. 5 SEM images of ZnO nanorods (plan and cross-sectional views) for different electrodeposition times, at 80°C, $[ZnCl_2]$=2.5mM, [KCl]=0.1M and E=-1V/SCE

This journal is © The Royal Society of Chemistry 20xx

Journal Name

ARTICLE

The stability of the structure is then enhanced by binding the latter with the Zn-polar plane (000$\bar{1}$) of new ZnO mesh. As a function of time, stability / instability process of ZnO polar facets contributes to a repetition of ZnO bonding along c axis at the atomic-scale leading to long nanorods at nanoscale (Fig. 7). The growth rate of ZnO is
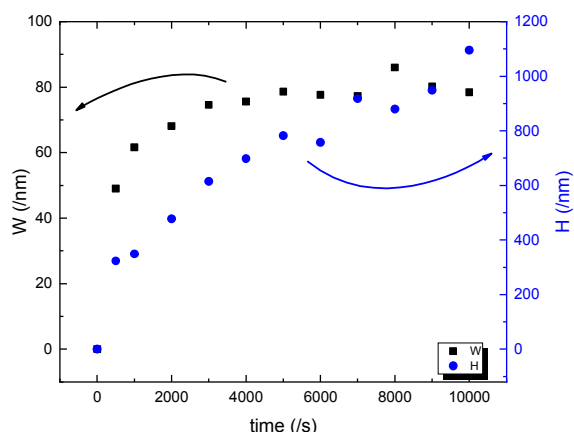

Fig. 6 Mean values of nanorod dimensions as a function of time, black squares for the width (W) and blue circles for the height (H).

mainly related to the plane polarity of growth direction. In fact, the deposition speed of ZnO oriented along Zn-polar plane is 1.5 times higher than ZnO oriented along O-polar plane.[32-35] The growth rate of ZnO in our case is relatively slow due to the O-polar plane (0001) which is responsible for growth along c axis.
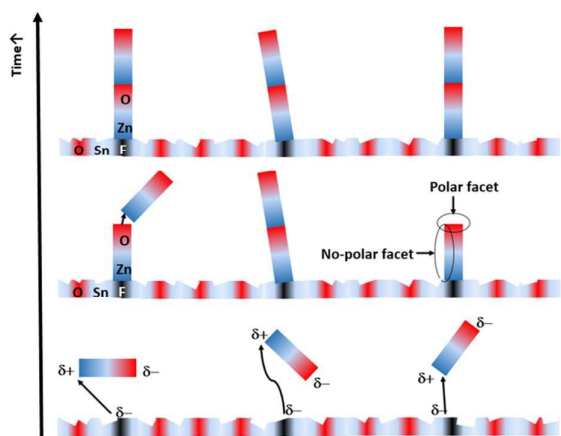

Fig. 7 Schematic illustration of ZnO growth mechanism for different synthesis times.

3.3 Effect of KCl concentration on ZnO nanorods growth on FTO

The effect of KCl concentration was carried out at constant temperature (80°C), time (1000s) and potential (-1V/SCE) of electrodeposition. The concentration of Zn^{2+} precursor is kept constant for all samples (2.5mM) and the KCl concentration varied

from 0.1 to 0.5M in the electrolyte solution saturated with oxygen. SEM images (Fig. 8) and estimated mass results (Table 3) show that the concentration of the electrolyte support, KCl, plays an inhibitor role on the ZnO electrodeposition when present in excess in the solution. The mass of ZnO electrodeposited on FTO and the density of ZnO nanorods decrease for a concentration of KCl higher than 0.5M.

[KCl] (/M)	Charge density (/C cm^{-2})	m(ZnO) (/µg)
0.1	0.144	61
0.5	0.154	65
1	0.138	58
2	0.130	55
3	0.126	53
4	0.097	41

Table 3 Estimated values of mass for ZnO nanorods electrodeposited for different support electrolyte concentrations.

Besides, the size of ZnO nanorods shows a significant growth at the level of the width and the height keeping the preferential direction of the growth according to c axis (Fig. 9).

On the one hand, the presence of KCl excess prevents ZnO nuclei from binding to the surface. This excess contributes to adsorption of K$^+$ and Cl$^-$ ions on the surface forming a barrier which impedes ZnO from depositing and weakens the polarity of the surface. Also, the adsorption of Cl$^-$ and K$^+$ on the surface causes a decrease of OH$^-$ around the surface contributing to a decrease of ZnO deposition rate. However, the first ZnO nuclei which appear near the surface bind to it and form a very attractive center for ZnO deposit (Fig. 10). Effect of KCl concentration on ZnO growth on FTO covered by nanocrystalline ZnO buffer layer has been reported by Tena-Zaera et al.[20] finding that the increase of KCl concentration mainly enhanced the longitudinal and lateral growth for a concentration of KCl higher than 1M. This result is also observed in our case. Tena-Zaera et al.[20] found also that an increase of KCl concentration causes an increase of ZnO deposition efficiency. This result is observed for a concentration lower than 0.5M. But high concentrations of KCl (>0.5M) cause a decrease of ZnO deposition efficiency.

Structurally, two main forms of ZnO nanorods can be distinguished according to the KCl concentration. The first one is ZnO nanorod arrays observed for a KCl concentration lower than 0.5M. For this form, ZnO nanorods retain the hexagonal form of ZnO with a flat end. The second one is ZnO nanopencil arrays observed for a KCl concentration higher than 0.5M. This form is generated by adsorption of K$^+$ ions on the O-polar plane of ZnO which weakens the
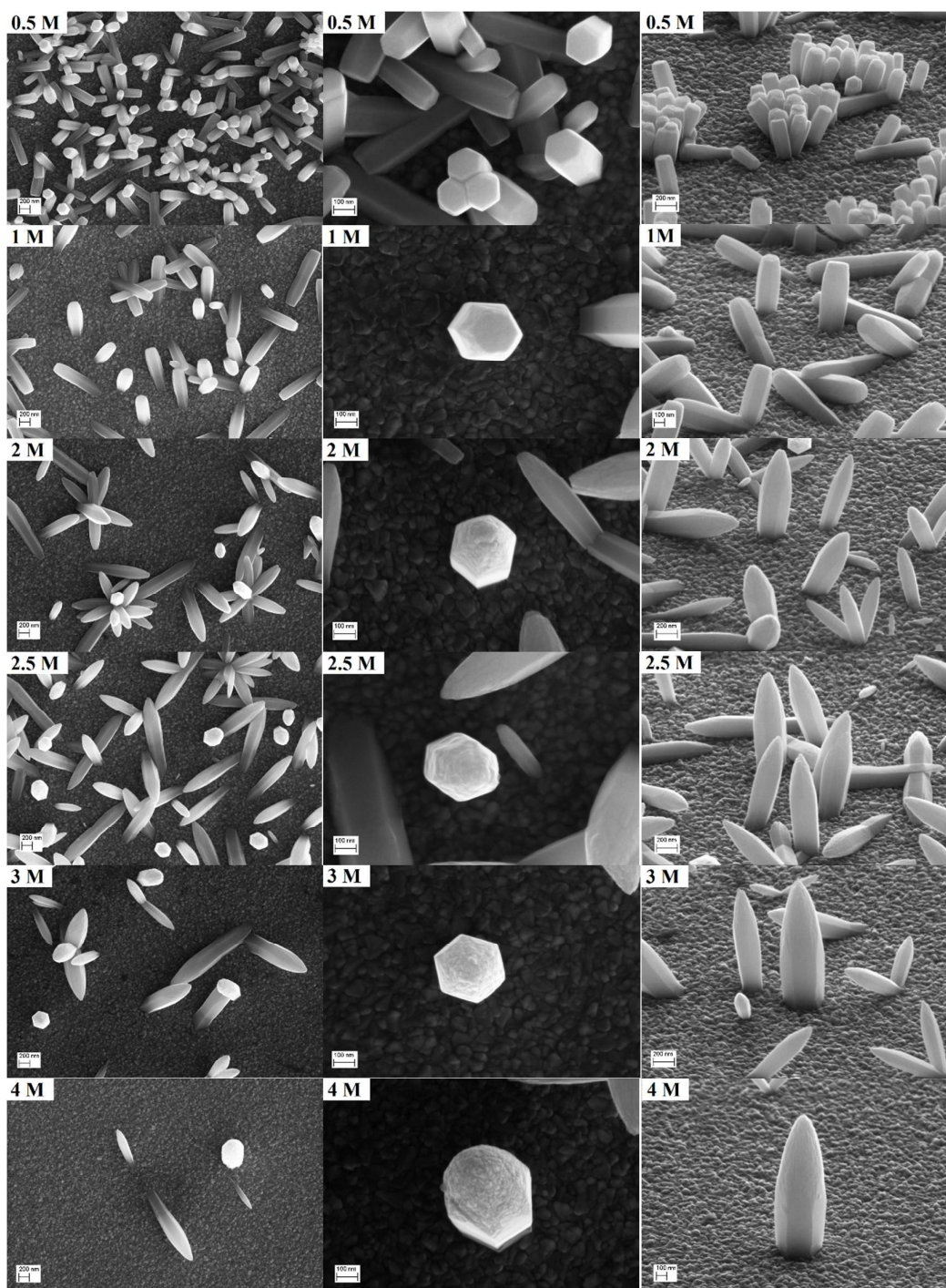
Journal Name

ARTICLE

Fig. 8 SEM images of ZnO nanorods (plan and cross-sectional view) for different KCl concentrations. T=80°C, [ZnCl$_2$]=2.5mM, time=1000s and E=-1V/SCE.
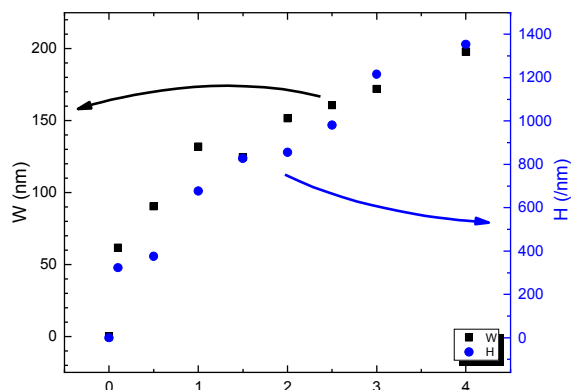
ARTICLE

Journal Name

Fig. 9 Mean values of nanorod dimensions as a function of KCl concentration, black square for the width (W) and blue circles for the height (H).

polarity of the plane (001) and prevents the natural growth of ZnO. The adsorption effect is more important on the edges than on the
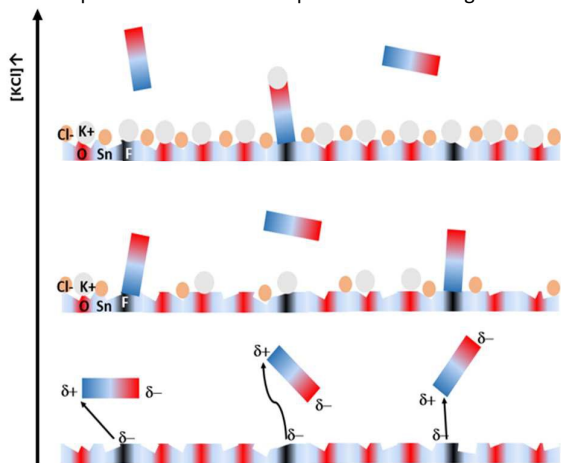

Fig. 10 Schematic illustration of ZnO growth mechanism for different concentrations of KCl.

center of ZnO nanorods. Xu *et al.*[26] reported the effect of the

adsorption of compounds other than KCl on the apparition of nanopencil arrays of ZnO.

3.4 Temperature effect on ZnO nanorods growth on FTO

From the same electrolyte solution saturated with oxygen made of $ZnCl_2$ (2.5mM) and KCl (0.1M), a series of sample was synthetized at the same potential (-1V/ SCE) and time (1000s) of electrodeposition but at various temperatures in the range of 30 to 80°C.

The temperature plays an important role on the ZnO formation. A precipitation of zinc hydroxide is promoted after oxygen reduction. The zinc hydroxide is thermodynamically unstable, a high temperature promotes their dehydration and therefore the ZnO formation.

The mass of ZnO electrodeposited on FTO surface increases with the temperature (Table 4). The rise in temperature leads also to an increase of ion mobility which promotes the ZnO deposition.

T (/°C)	Charge density (/C cm^{-2})	m(ZnO) (/µg)
30	0.032	13
40	0.106	45
50	0.137	58
60	0.138	58
70	0.181	76
80	0.204	86

Table 4 Estimated values of mass for ZnO nanorods electrodeposited at various temperatures

The SEM images (Fig. 11) show the temperature effect on ZnO growth on FTO. As a function of temperature, the thin film of ZnO changes its appearance from a smooth thin film to nanostructure thin film, through randomly structures. For temperatures between 40 to 50°C, ZnO growths on the surface as small grains having a rough wall. For temperature between 50 to 70°C, ZnO nanorods begin to appear, but with a rough wall. For temperature equal to 80°C, the hexagonal nanorods of ZnO grows with smooth walls and marked crystalline plans.
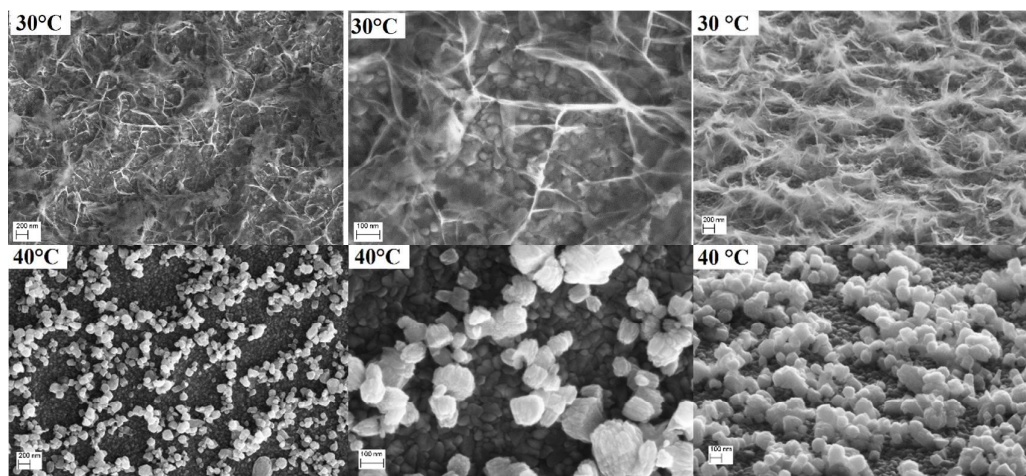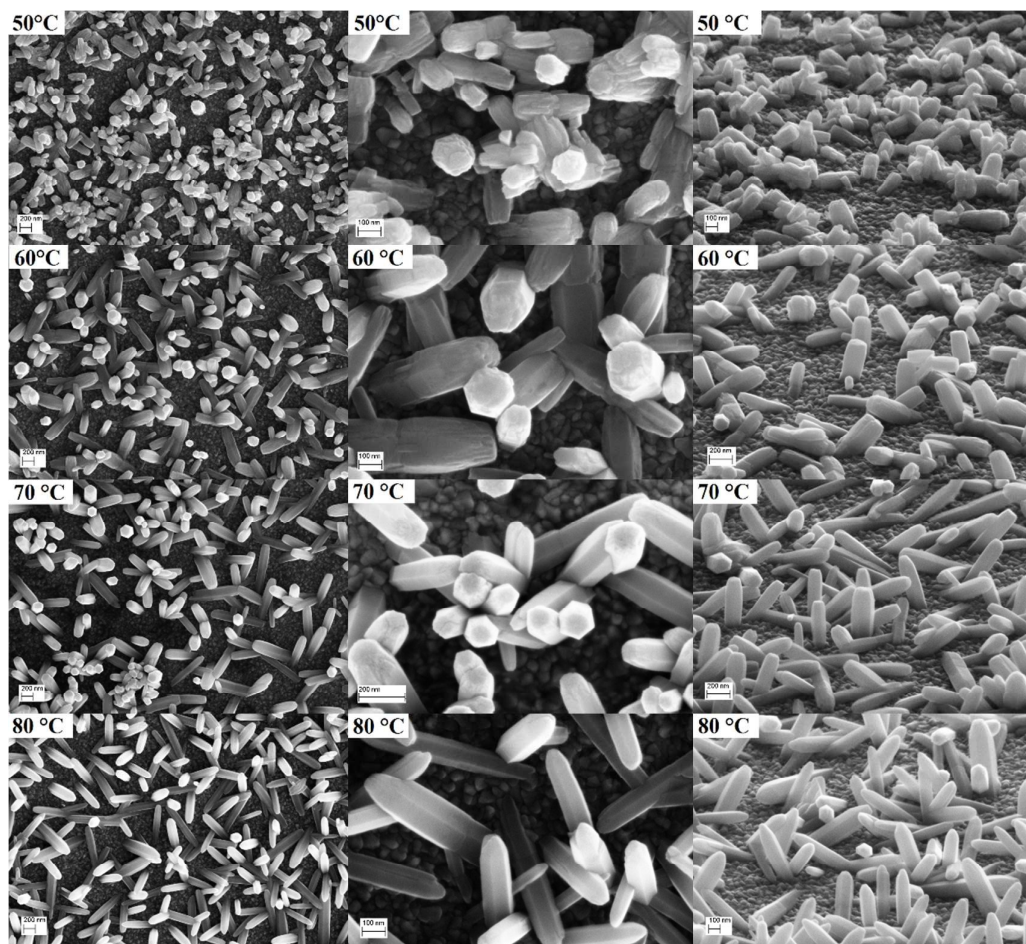
Fig. 11 SEM images of ZnO nanorods (plan and cross-sectional view) for different temperatures. Time=1000s, [ZnCl$_2$]=2.5mM, [KCl]=0.1M and E=-1V/SCE.

The XRD patterns results of ZnO nanostructured thin films showed that only at 80°C, ZnO was crystallized under Wurtzite crystal structure. The Wurtzite crystal structure is identified by (100), (002),
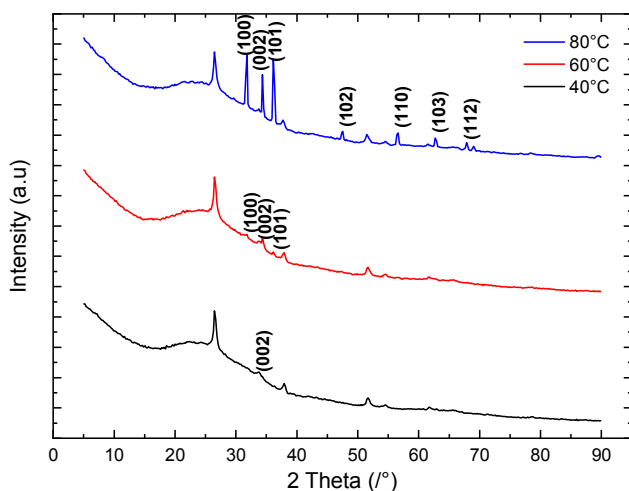

Fig. 12 XRD patterns of ZnO synthesized at 40, 60, and 80°C

(101), (102), (110), (103), (200) and (112) crystal planes locating at 2θ

values of 31.8°, 34.4°, 36.3°, 47.5°, 56.6°, 62.9°, 66.4°, and 68.0°, respectively.

Moreover, the peaks at 2θ values of 27° and 52° correspond to FTO crystal structure (Fig. 12). These results agreed with several works which have studied the temperature effect on crystallization of material[23, 24] finding that high temperatures give rise to a good crystallization of the material. Moreover, in our case, we can notice that the intensities of (100) and (101) planes are higher than this of (002). This is related to the surface roughness and especially to the inclination of ZnO nanorods revealing the most hydrophobic planes as mentioned by Chang *et al.*[36]

4. Conclusion

The electrodeposition in one step of ZnO nanorods on FTO is carried out under different conditions. The effect of four main parameters (concentration of Zn^{2+} precursor, time of electrodeposition, concentration of supporting electrolyte and temperature of electrodeposition) on the ZnO growth is studied. The concentration of Zn^{2+} precursor mainly plays a role on the density of nanorods. A high concentration of Zn^{2+} precursor causes a high nucleation rate around the fluorine atoms of the surface leading to nanoflower-like structures after growth process (Fig. 13 (a)). The electrodeposition

ARTICLE   **Journal Name**

time of ZnO mainly influences the height of nanorods (Fig. 13 (b)). Moreover, the temperature is an important parameter regarding the transfer of matter in the electrolyte and the appearance of ZnO nanorods with accented crystalline planes (Fig. 13 (c)). Finally, the concentration of KCl influences the nanorods density. A high concentration gives rise to a low density of nanorods. However, a high temperature increases the conductivity of the solution and promotes the dehydration of zinc hydroxide guaranteeing the
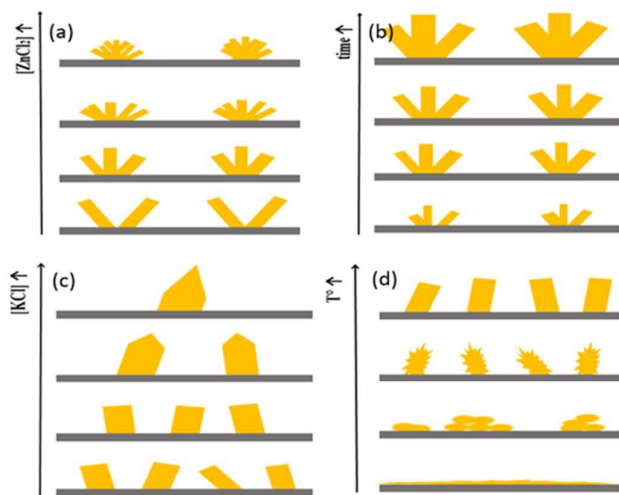

Fig. 13 Schematic view of ZnO growth on FTO under different conditions; (a) $ZnCl_2$ concentration, (b) time, (c) KCl concentration and (d) temperature.

electrochemical deposition of ZnO (Fig. 13 (d)).

Conflicts of interest

There are no conflicts to declare.

Acknowledgements

References

1   M. Sasani Ghamsari, S. Alamdari, W. Han and H.-H. Park, *Int. J. Nanomedicine*, 2017, **Volume 12**, 207-216.

2   R. Pietruszka, B. S. Witkowski, S. Gieraltowska, P. Caban, L. Wachnicki, E. Zielony, K. Gwozdz, P. Bieganski, E. Placzek-Popko and M. Godlewski, *Sol. Energy Mater. Sol. Cells*, 2015, **143**, 99-104.

3   D. N. Papadimitriou, *Thin Solid Films*, 2016, **605**, 215-231.

4   A. Henni, A. Merrouche, L. Telli, A. Karar, F. I. Ezema and H. Haffar, *J. Solid State Electrochem.*, 2016, **20**, 2135-2142.

5   A. Tello, H. Gomez, E. Munoz, G. Riveros, C. J. Pereyra, E. A. Dalchiele and R. E. Marotti, *J. Electrochem. Soc.*, 2012, **159**, D750-D755.

6   C. Badre, T. Pauporte, M. Turmine and D. Lincot, *Nanotechnology*, 2007, **18**, 4.

7   J. Kennedy, P. P. Murmu, J. Leveneur, V. M. Williams, R. L. Moody, T. Maity and S. V. Chong, *J. Nanosci. Nanotechnol.*, 2018, **18**, 1384-1387.

8   K. Kaviyarasu, C. Maria Magdalane, K. Kanimozhi, J. Kennedy, B. Siddhardha, E. Subba Reddy, N. K. Rotte, C. S. Sharma, F. T. Thema, D. Letsholathebe, G. T. Mola and M. Maaza, *J. Photochem. Photobiol. B*, 2017, **173**, 466-475.

9   J. Kennedy, F. Fang, J. Futter, J. Leveneur, P. P. Murmu, G. N. Panin, T. W. Kang and E. Manikandan, *Diamond Relat. Mater.*, 2017, **71**, 79-84.

10   J. Kennedy, P. P. Murmu, J. Leveneur, A. Markwitz and J. Futter, *Appl. Surf. Sci.*, 2016, **367**, 52-58.

11   J. Kennedy, P. P. Murmu, E. Manikandan and S. Y. Lee, *Journal of Alloys and Compounds*, 2014, **616**, 614-617.

12   J. Kennedy, A. Markwitz, Z. Li, W. Gao, C. Kendrick, S. M. Durbin and R. Reeves, *Current Applied Physics*, 2006, **6**, 495-498.

13   A. R. Khataee, A. Karimi, R. D. C. Soltani, M. Safarpour, Y. Hanifehpour and S. W. Joo, *Applied Catalysis A: General*, 2014, **488**, 160-170.

14   K. C. Sekhar, A. Khodorov, A. Chahboun, S. Levichev, A. Almeida, J. A. Moreira, K. Kamakshi, C. J. R. Silva, M. Pereira and M. J. M. Gomes, *Mater. Chem. Phys.*, 2012, **135**, 174-180.

15   H. Ghannam, Z. O. El Hmaidi, Z. Y. Alami, M. Addou, A. Chahboun, M. Salem and M. Gaidi, International Renewable and Sustainable Energy Conference (IRSEC), Ouarzazate, MOROCCO, 2014.

16   N. Kıcır, T. Tüken, O. Erken, C. Gumus and Y. Ufuktepe, *Appl. Surf. Sci.*, 2016, **377**, 191-199.

17   H. Zhang, S. Jin, G. Duan, J. Wang and W. Cai, *J. Mater. Sci. Technol.*, 2014, **30**, 1118-1123.

18   G. Nagaraju, Y. H. Ko and J. S. Yu, *Mater. Chem. Phys.*, 2015, **149-150**, 393-399.

19   M. Skompska and K. Zarębska, *Electrochim. Acta*, 2014, **127**, 467-488.

20   R. Tena-Zaera, J. Elias, G. Wang and C. Levy-Clement, *J. Phys. Chem. C*, 2007, **111**, 16706-16711.

21   J. Elias, R. Tena-Zaera and C. Levy-Clement, *J. Phys. Chem. C*, 2008, **112**, 5736-5741.

22   J. Elias, R. Tena-Zaera and C. Lévy-Clément, *J. Electroanal. Chem.*, 2008, **621**, 171-177.

23   D. Pradhan and K. T. Leung, *J. Phys. Chem. C*, 2008, **112**, 1357-1364.

24   A. Goux, T. Pauporté, J. Chivot and D. Lincot, *Electrochim. Acta*, 2005, **50**, 2239-2248.

25   C. Badre, P. Dubot, D. Lincot, T. Pauporte and M. Turmine, *J. Colloid Interface Sci.*, 2007, **316**, 233-237.

26   L. F. Xu, Y. Guo, Q. Liao, J. P. Zhang and D. S. Xu, *J. Phys. Chem. B*, 2005, **109**, 13519-13522.

27   S. H. Lee, T. Minegishi, J. S. Park, S. H. Park, J. S. Ha, H. J. Lee, H. J. Lee, S. Ahn, J. Kim, H. Jeon and T. Yao, *Nano Lett.*, 2008, **8**, 2419-2422.

28   G. Perillat-Merceroz, P. H. Jouneau, G. Feuillet, R. Thierry, M. Rosina and P. Ferret, *Journal of Physics: Conference Series*, 2010, **209**, 012034.

29   A. Goux, T. Pauporté and D. Lincot, *Electrochim. Acta*, 2006, **51**, 3168-3172.

30   B. B. Li, U. Philipose, C. F. de Souza and H. E. Ruda, *J. Electrochem. Soc.*, 2011, **158**, D282.

Please do not adjust margins

Journal Name

ARTICLE

31   K. Ichinose, T. Mizuno, M. Schuette White and T. Yoshida, *J. Electrochem. Soc.*, 2014, **161**, D195-D201.

32   X. Wang, Y. Tomita, O.-H. Roh, M. Ohsugi, S.-B. Che, Y. Ishitani and A. Yoshikawa, *Appl. Phys. Lett.*, 2005, **86**, 011921.

33   H. Kato, M. Sano, K. Miyamoto and T. Yao, *J. Cryst. Growth*, 2005, **275**, e2459-e2465.

34   J. S. Park, J. H. Chang, T. Minegishi, H. J. Lee, S. H. Park, I. H. Im, T. Hanada, S. K. Hong, M. W. Cho and T. Yao, *J. Electron. Mater.*, 2007, **37**, 736-742.

35   J. S. Park, T. Minegishi, J. W. Lee, S. K. Hong, J. H. Song, J. Y. Lee, E. Yoon and T. Yao, *J. Appl. Phys.*, 2010, **107**, 123519.

36   S.-Y. Chang, N.-H. Yang and Y.-C. Huang, *J. Electrochem. Soc.*, 2009, **156**, K200.

CrystEngComm Accepted Manuscript

Please do not adjust margins
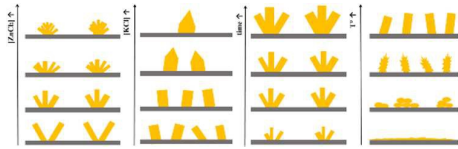
Effect of four parameters on the ZnO growth onto FTO